Supporting Information

Targeted synthesis of gold nanorods and characterization of their tailored surface properties using X-ray and optical spectroscopy

David G. Schauer,[ab] Jona Bredehoeft,[a] Umar Yunusa,[b] Ajith Pattammattel,[c] Hans Jakob Wörner,[a] Emily A. Sprague-Klein*[b]

[a] *ETH Zurich, Dept. of Chemistry and Applied Biosciences, Laboratory of Physical Chemistry, Vladimir-Prelog-Weg 2 (HCI E 241), 8093 Zürich, Switzerland.*
[b] *Department of Chemistry, Brown University, Providence, Rhode Island 02912, USA. Tel: +1 (401) 863 3586; E-mail: emily_sprague-klein@brown.edu*
[c] *National Synchrotron Light Source II, Brookhaven National Laboratory, Upton, NY 11973, USA*

Contents

1 Extended experimental **2**
1.1 Chemicals . . . 2
1.2 General procedure . . . 2
1.2.1 Growth solution . . . 3
1.2.2 Seed solution (SeSo) . . . 3
1.2.3 Combination of SeSo and GS . . . 4
1.2.4 Recovery of the GNRs . . . 4
1.2.5 Preparation of GNR samples for Microscopy Analyses . . . 4
1.3 Synthesis of gold nanorods (GNRs) . . . 4
1.4 Synthesis of gold nanospheres (GNSs) . . . 5
1.5 Purity- and vendor-dependent synthesis . . . 6

2 Voigt-fit procedure **7**

3 Raw data of 2D-XANES spectra recorded at 3-ID Hard X-ray Nanoprobe **8**

1 Extended experimental

1.1 Chemicals

The chemicals used for the different synthesis procedures are listed in Tbl. 1. These were applied and stored without further purification and at room temperature (25 °C). $HAuCl_4 \cdot 3H_2O$ was stored at 7 °C in a chemical refrigerator. Milli-Q water (18.2 MΩ·cm at 25 °C) was used for all solution preparations and the synthesis procedures.

Table 1 The chemical name, the common abbreviation, and the manufacturer of the chemicals used within the experiments are listed

Chemical name	Abbreviation	Vendor
Cetyltrimethyl ammonium bromide	CTAB	Sigma, Merck, TCI
Hydroxylamin hydrochlorid	$NH_2OH \cdot HCl$	Sigma
Hydrogen tetrachloroaurate(III) trihydrate	$HAuCl_4 \cdot 3H_2O$	abcr., Sigma
Silver nitrate	$AgNO_3$	Brenntag Schweizerhall AG, Sigma
Sodium borohydride	$NaBH_4$	Sigma, Merck
Sodium hydroxide	NaOH	Sigma, VWR Chemicals

1.2 General procedure

The procedure for the seed-mediated synthesis was primarily guided by the method described by Leng et al.[1] In this chapter, the general synthesis process for gold nanoparticles (GNPs) is explained step by step. In the chapters 1.3, 1.4 and 1.5, the specific requirements for the synthesis of both gold nanorods (GNRs) and gold nanospheres (GNSs) are addressed.

The synthesis process is broken down into its essential substeps in the following subsections, shown in Fig. 1. First, the synthesis of the pH-controlled growth solution (GS) is described, which is to be prepared simultaneously with the seed solution (SeSo) required for initiating the growth process of the GNRs and GNSs. These two solutions are combined as a final step in the synthesis process, and the growth is initiated under controlled temperature and time conditions. Finally, the prepared nanoparticles are recovered after the surfactant (CTAB) is removed by centrifugation.

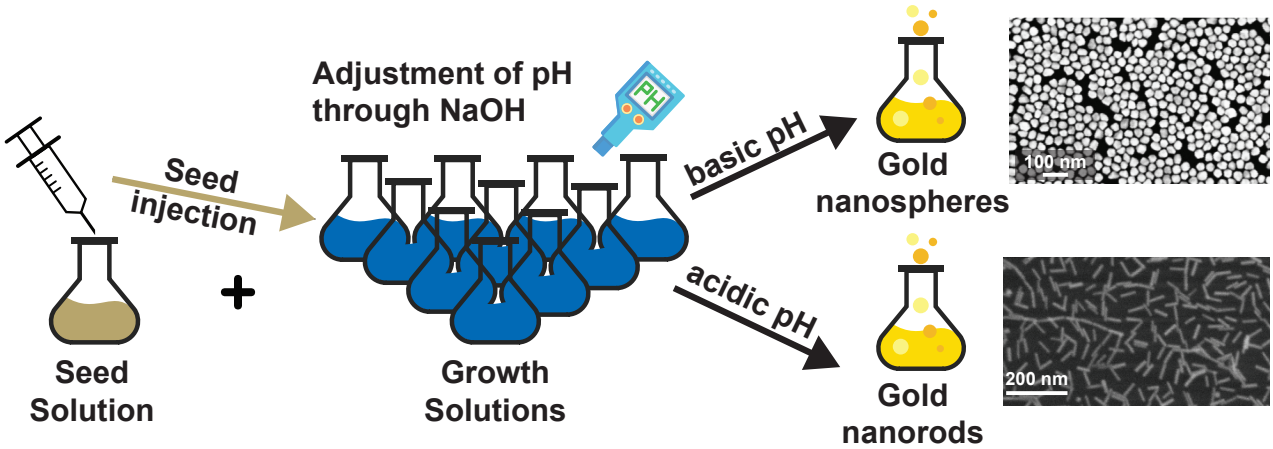

Figure 1 Scheme of the experimental procedure leading to the growth of (an)isotropic gold nanoparticles.

1.2.1 Growth solution

To prepare the GSs the chemicals CTAB, $HAuCL_4 \cdot 3H_2O$, $AgNO_3$, $NH_2OH \cdot HCl$ and NaOH from Tbl. 1 were used. To ensure accurate weighing and better reproducibility and comparability, stock solutions of 100 mL each were prepared in Milli-Q water and stored in a constantly heated water bath of exactly 28 °C. In Tbl. 2, the required concentrations, molar masses, and weighed-in masses are listed.

Table 2 The concentration, molar mass, and required mass of the chemicals for the preparation of 100 mL stock solutions are shown. The mass was rounded to two significant digits

Chemical	c / (mol · L^{-1})	M / (g · mol^{-1})	m / g
$HAuCL_4 \cdot 3H_2O$	$5 \cdot 10^{-3}$	393.8	0.20
$AgNO_3$	0.01	169.873	0.17
$NH_2OH \cdot HCl$	0.1	69.49	0.69
CTAB	0.2	364.4	7.3
NaOH	0.2	39.997	0.80

The GSs were prepared in 20 mL screwable glass vials, and a suitable stirring bar was added. The desired amounts of the stock solution were extracted using sterile needles and syringes or micro-liter pipettes with a suitable volume. Throughout the synthesis, the glass vials were placed on a magnetic stirrer, with which the solutions were mixed at a constant speed of 300 - 400 rpm. Per GS, 5 mL of the stock solution of CTAB were mixed with 0.1 mL of the stock solution of $AgNO_3$. Then 5 mL of the stock solution of $HAuCl_4 \cdot 3H_2O$ ($5 \cdot 10^{-3}$ mol · L^{-1}) were added. Once the solution got a uniform, transparent color of yellow-gold, 5 mL of the stock solution of $NH_2OH \cdot HCl$ were added. A color change from yellow-gold to colorless-transparent was observed within a few minutes. Once this had happened, the pH was measured using a pH meter. The pH should be strongly acidic at about 2.70 ± 0.20. Then, according to the synthesis goals, the pH was increased using the stock solution of NaOH. This was implemented using a glass Pasteur pipette and adding NaOH drop per drop while constantly measuring the pH. As soon as the pH is within the desired range, the magnetic stirrer can be switched off, the stirring bar removed, and the lid screwed. The GSs were now ready for the addition of the SeSo and were stored in a 28 °C water bath until seeding, which needs to be completed <5 min after the pH adjustment.

1.2.2 Seed solution (SeSo)

The SeSos were prepared in 20 mL screwable glass vials with a suitable stirring bar. As described in Leng et al.[1], the SeSos should be used freshly. During this work, the SeSos were disposed of after 30 min at the latest, and new SeSos were prepared. Also, three SeSos were simultaneously synthesized, so a direct comparison of color and pH value was possible. To prepare the SeSos, the chemicals CTAB, $HAuCl_4 \cdot 3H_2O$, and $NaBH_4$ from Tbl. 1 were utilized. As in section 1.2.1, 100 mL stock solutions in Milli-Q water were prepared. In Tbl. 3, the required concentrations, molar masses, volumes, and weighed-in masses are listed. The stock solution for CTAB is identical to the previous one. The stock solution of $HAuCl_4 \cdot 3H_2O$ is diluted by a factor of ten compared to the one used for the GSs and was newly made. The stock solution of $NaBH_4$ was cooled using an ice-ice-water bath and was discarded after one hour.

Using a suitable syringe and metal needle (or pipette) 5 mL of the stock solution of CTAB were added to the glass vial and stirred at 300 rpm together with 5 mL of the stock solution of $HAuCl_4 \cdot 3H_2O$ ($5 \cdot 10^{-4}$ mol · L^{-1}). Once the solution had turned to an intense golden-yellow color (<1 min), the magnetic stirrer was set to 800 rpm, and 0.60 mL of the ice-cooled stock solution of $NaBH_4$ was added

Table 3 The concentration, molar mass, and required mass of the chemicals for the preparation of 100 mL stock solutions are shown. The mass was rounded to two significant digits

Chemical	c / (mol · L^{-1})	M / (g · mol^{-1})	m / g
$HAuCL_4 \cdot 3H_2O$	$5 \cdot 10^{-4}$	393.8	0.020
$NaBH_4$	0.01	37.84	0.038

rapidly in one go. The mixture immediately took on a brown-transparent color. After stirring for about five minutes, the stirring bar was removed, the glass vial was screwed, and the SeSos were ready to be used (<30 min).

1.2.3 Combination of SeSo and GS

Using a microlitre syringe (volume: 2 µL - 20 µL), precisely 15 µL were added to each GS. The lids were then screwed back on, and the GS was placed in the 28 °C water bath. Depending on the pH value, the colorless GSs changed to an intense blue-violet or yellow-gold and pink, or an intense dark red was observed after approximately one hour.

1.2.4 Recovery of the GNRs

Once the desired growth time was reached, the seeded GSs were removed from the water bath. The absorption wavelengths of the GNRs were measured with a UV/Vis/NIR absorption spectrometer, using either a *BRAND* 1.5 mL (12.5 x 12.5 x 45 mm) disposable or a *SPECTROCELL* 0.7 mL (2 mm) Quartz cuvette.

Subsequently, the individual solutions were transferred into screwable, conical 15 mL centrifugation tubes and centrifuged for 15 - 25 min (depending on the shape and size) at 5500 - 6000 rpm. Thus, unreacted chemicals can be removed, and the growth process is terminated. After an additional centrifugation cycle, the purified GNRs were stored at room temperature for further use.

1.2.5 Preparation of GNR samples for Microscopy Analyses

To prepare the GNRs for further experiments, they were deposited on ultra-thin silicon nitride (Si_3N_4) membranes stretched on silicon frames (thickness of 30 nm or 100 nm) or onto pre-cut silicon wafers (5 x 5 x 0.67 mm). The membranes were separately glued on silicon plates and subsequently mounted onto a suitable scanning electron microscope pin stub (12 mm diameter) using UV glue to facilitate the depositions and further imaging analyses. Before the GNPs were applied to the surfaces, the membranes were treated with a UV-Ozone cleaner; thus, the liquid could spread homogeneously on the surfaces. A treatment of 5 - 10 min was sufficient. Since this effect of hydrophilisation does not last long (<5 min), the GNPs were applied as quickly as possible onto the treated membranes using either a spin coater or drop-casting. 10 - 20 µL of the very concentrated GNP solutions were applied very carefully with the aid of a microlitre syringe. After the water evaporates, another drop can be applied if necessary. It was found that the Milli-Q water with a high concentration of GNPs was very well distributed over the entire membrane surface. These membranes were then examined with either a scanning or transmission electron microscope. Subsequently, the membranes were carefully detached from the SEM plates with acetone or a very sharp scalpel.

1.3 Synthesis of gold nanorods (GNRs)

In this section, the specific synthesis of GNRs is described. The individual steps were implemented chronologically as described in section 1.2 and adapted to the conditions for the synthesis of GNRs. Fig. 2 shows the absorption spectra of GNRs having a variety of different aspect ratios.

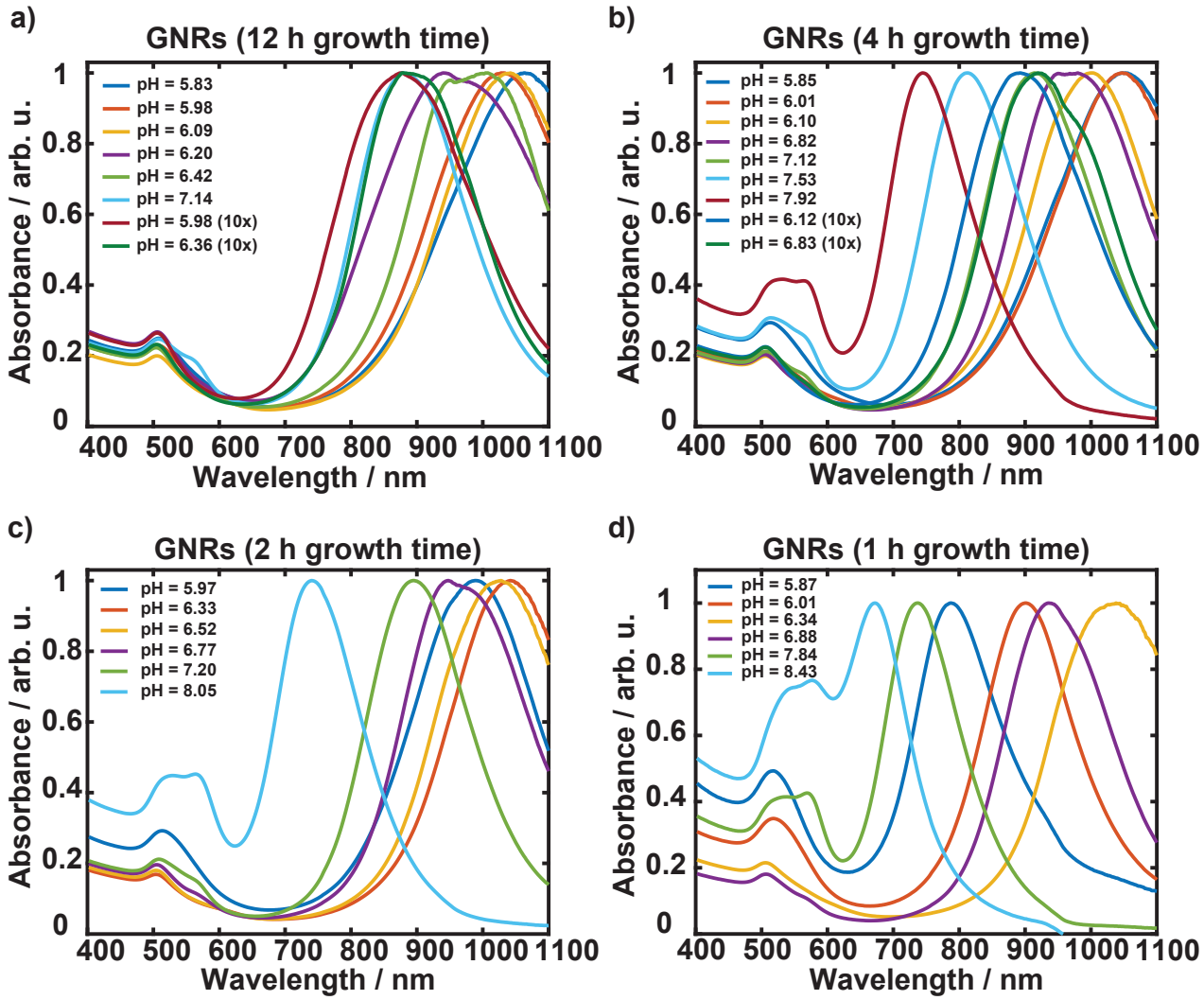

Figure 2 a), b), c), d) The normalized absorption (resonance) spectra of the synthesized GNRs with a growth time of 12 h, 4 h, 2 h, and 1 h showing two distinct peaks, corresponding to the radius (≈500 nm peaks) and the length (<700 nm peaks) of the GNRs.

The instructions for synthesizing the GSs and the SeSos described in the sections 1.2.1 and 1.2.2 were applied identically for synthesizing GNRs. The critical factor for obtaining rods is adjusting the pH value in the different GSs. Almost exclusively nanorods were formed in the acidic pH region of about 5 - 7. No more distinct rods were formed if the pH value approaches the neutral to slightly basic regime (≈8.5). The length of the rods was decreased with an increase in the pH. The diameter of the GNRs was consistent and not changed throughout the synthesis process. As the neutral to slightly basic pH range was reached, the diameter became more prominent, and the nanorods were misshapen and could not be characterized as typical "rods". The remaining steps of the general procedure were executed as described beforehand.

1.4 Synthesis of gold nanospheres (GNSs)

In this section, the specific synthesis of GNSs is described. The individual steps were implemented chronologically as in section 1.2 and adapted to the conditions for the synthesis of GNSs. The instructions for the syntheses of the GSs and the SeSos described in the sections 1.2.1 and 1.2.2 were applied

identically for the production of the GNSs. The critical factor for obtaining spheres is adjusting the pH value in the different GSs. Almost exclusively nanospheres were formed in the basic pH region (>9). If the pH approaches the neutral regime (≈8), no more distinct spheres were formed, and in the absorbance spectrum two distinct peaks ("rod-like" shape, anisotropy) instead of one have become more and more visible. The remaining steps of the general procedure were executed as described beforehand.

1.5 Purity- and vendor-dependent synthesis

Fig. 3 shows five different graphs of absorption spectra of gold nanoparticles. We exchanged the supplier and the purity of the used CTAB and monitored the changes in the LSPR of the nanoparticles. One can clearly state that the higher purity actually led to a less satisfying result, meaning either the formation of only isotropic nanoparticles (one LSPR peak) or a broadened full-width-half-maximum of the LSPW. The most pleasing result was achieved with the CTAB having a purity of 98% — the nanoparticles in these figures were not used for further analysis. In the case of unsatisfactory reproducibility, non-degraded chemicals might be prudent.

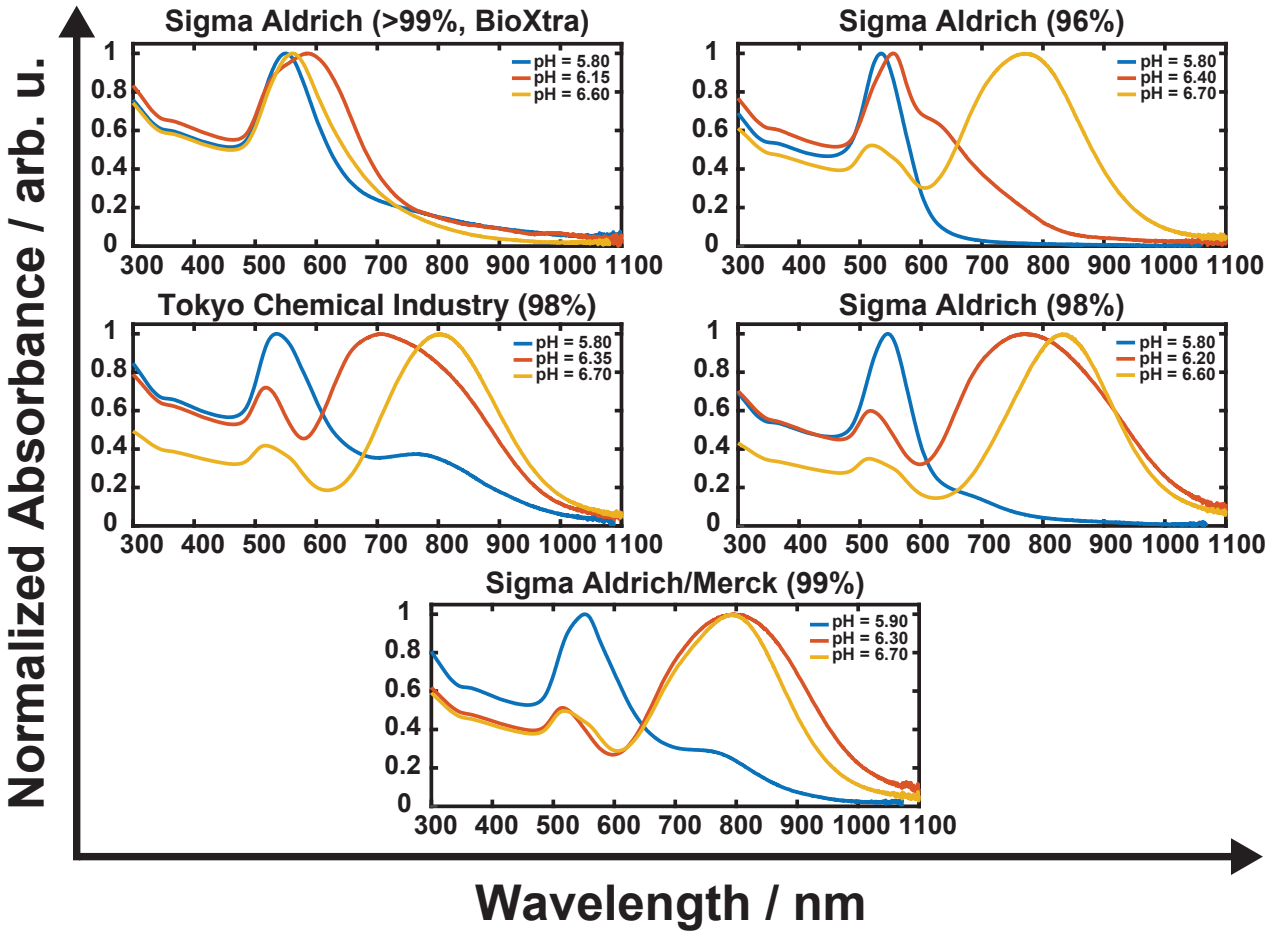

Figure 3 The absorption spectra (24 h growth time) of GNRs using the synthesis method described above using five different CTAB suppliers and purities leading towards different results.

2 Voigt-fit procedure

This section provides an overview of the fitting algorithm for analyzing the absorption data obtained from the synthesized GNRs. The algorithm utilizes three Voigt peaks and a power law to model the absorption peaks resulting from the length of the rods and their diameter, as well as an additional peak to account for the presence of spherical nanoparticles, if applicable. The fitting algorithm extracted the absorption peak center from the spectra shown in Fig. 2. For all fits, the following mathematical model was used

$$f(E) = c + a_0 \cdot E^b + \sum_{i=1}^{3} a_i \cdot V_{norm}(E, \mu_i, \sigma_i, \Gamma_i). \tag{1}$$

In this equation, E is the energy, c is a constant, a_0 and b describe the non-resonant absorption modeled by a power law and a_i is the scaling factor for the normalized Voigt peaks (V_{norm}), with

$$V(E, \mu, \sigma, \Gamma) = \frac{1}{\sigma \cdot \sqrt{2\pi}} \cdot \mathrm{Re}\left[w(z)\right], \tag{2}$$

where $w(z)$ is the *Faddeeva function* (a complex scaled complex complementary error function).[2,3] The employed fitting algorithm is making use of the Matlab implementation of the Faddeeva function.[4] The data and their corresponding fits are shown in Fig. 4. The overall agreement appears to be decent. For the more blueshifted spectra, the power law does not capture the non-resonant absorption very well, resulting in slight deviations that may lead to small errors in the obtained peak value. A reason for this could be the inherent skewness of the particle distribution for those spectra.

In conclusion, by utilizing this algorithm, we successfully extracted essential information related to the GNRs' length distribution, width variation, and the presence of spherical nanoparticles.

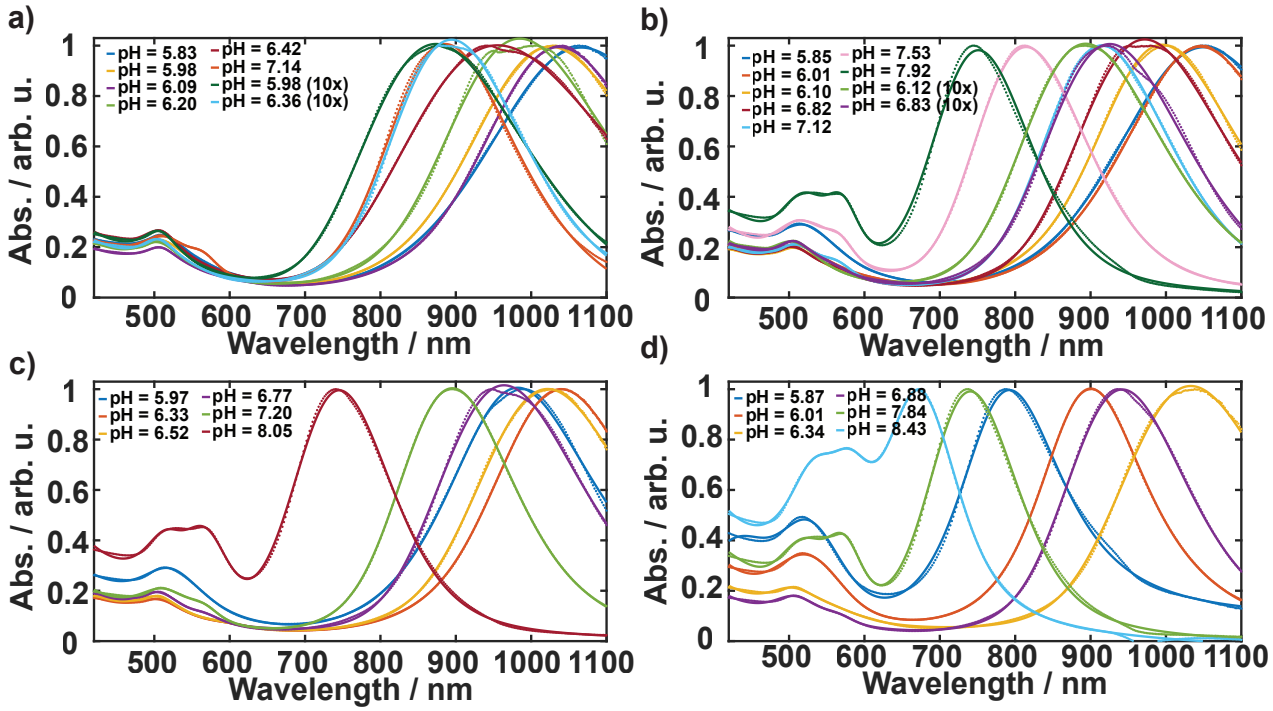

Figure 4 a), b), c), d) The absorption spectra from Fig. 2 showing the data (dotted line) and fit result (solid line).

3 Raw data of 2D-XANES spectra recorded at 3-ID Hard X-ray Nanoprobe

Fig. 5 shows the raw data and the first derivative of the recorded 2D X-ray absorption near-edge structure (2D-XANES) data used in the main manuscript. In Fig. 5b, a redshift can be observed between the spectra of the GNRs with a resonance at 772 nm in comparison to the gold foil and the GNRs with a resonance at 706 nm.

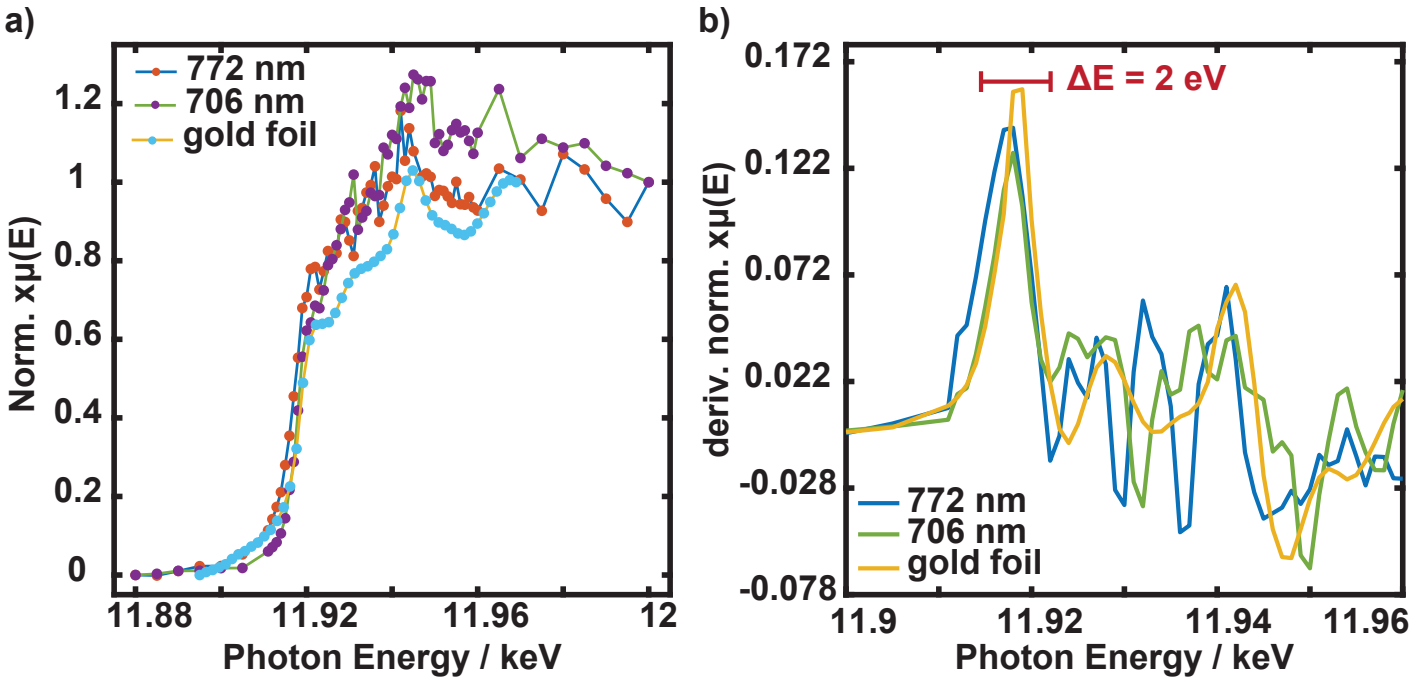

Figure 5 a) The raw data of the recorded 2D-XANES. **b)** The first derivative of the spectra from a).

In Fig. 6, the 2D-XANES spectra for the 772 nm sample are plotted using different sizes of the ROI in the 2D X-ray fluorescence (2D-XRF) maps. Using the smallest ROI size (5 x 5 px^2, 200 x 200 nm^2), the signal-to-noise ratio of the processed 2D-XANES resulted in the highest intensity and, more importantly, yielding the highest resolution, especially of the post-edge oscillatory features, giving the best results for further analysis. A possible explanation for this could be that the investigated particles have a length of ≈60 nm and a diameter of ≈20 nm. In contrast, the resolution of the X-ray beam was only 40 nm, resulting in the best signal-to-noise when excluding the noisy background regions in the image.

Fig. 7a shows a similar approach to the one presented in Fig. 6, trying to optimize the signal-to-noise ratio and determining whether the post-edge oscillations are actual features or relics of noise. Hereby, the highest intensity regions (photon-count/pixel) from the 2D-XRF maps were extracted using an ROI of 5 x 5 px^2 and accumulated (presented by the black dashed spectrum). The orange spectrum represents that spectrum's "three-point smoothing" with only one repetition, the same method used for the spectra in Fig. 3 in the main manuscript. It can be observed that the peak at 11.395 keV is still present and not a noise-resulting feature. In Fig. 7b, the comparison of two regions on the 2D-XRF (ROI of 5 x 5 px^2) maps is displayed. The orange spectrum corresponds to the in-focus region yielding the highest intensity (adjusted before the measurement). In contrast, the green spectrum was processed from the off-focus region of the 2D-XRF maps, resulting in little intensity and resolution due to the lack of particle concentration.

A more detailed description of the beamtime (3-ID HXN) and the data acquisition and analysis can be found in Pattammattel et al.[5,6]

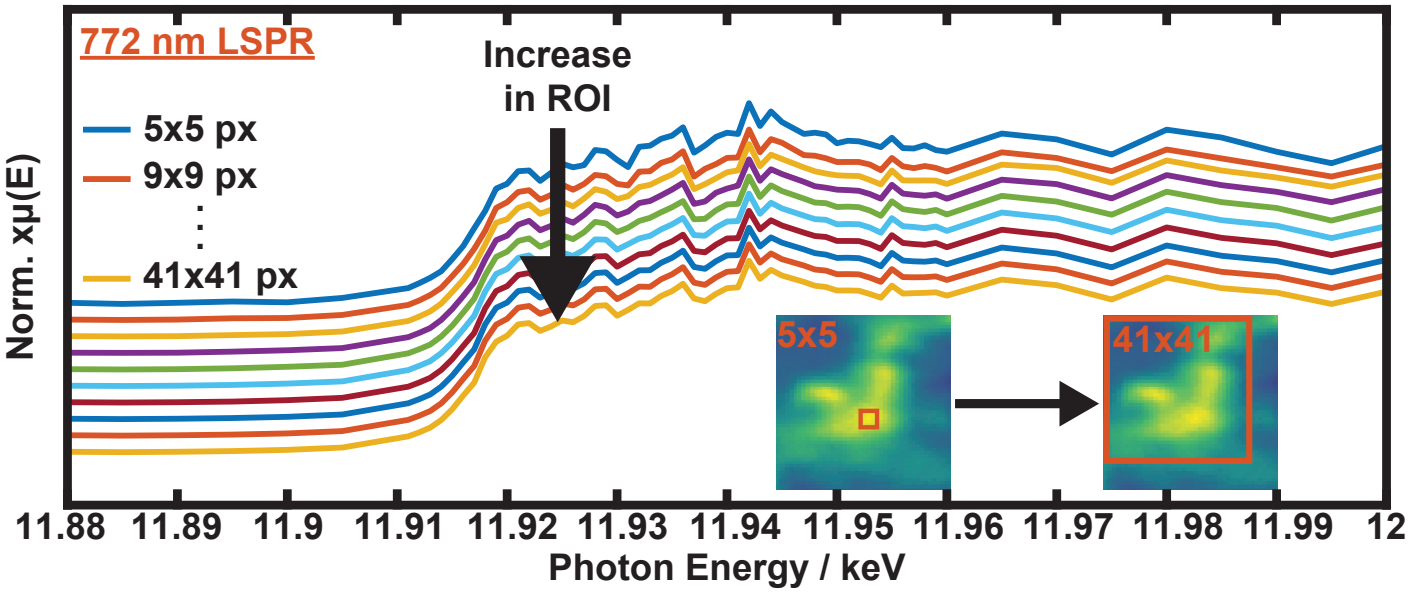

Figure 6 Increase of the ROI in the 2D-XRF maps subsequently decreased the observed intensity in the processed 2D-XANES spectra. All these spectra were normalized and stacked to compare the post-edge oscillatory features. The y-axis offset can be neglected and was chosen arbitrarily.

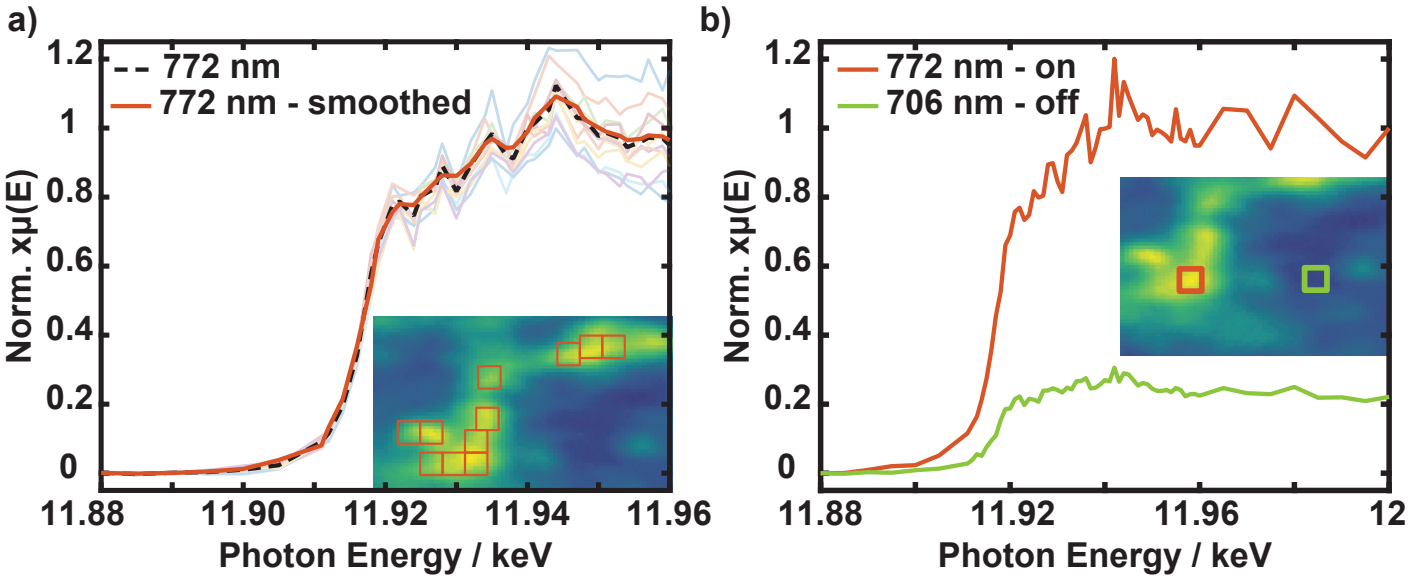

Figure 7 a) The accumulated spectrum of eleven ROI (5 x 5 px^2) extracted from the regions showing the highest particle concentration (intensity). **b)** The difference in the spectrum when processed from focused high particle concentration (high intensity) regions compared to the out-of-focus low concentration (low intensity) regions.

References

[1] Y. Leng, X. Yin, F. Hu, Y. Zou, X. Xing, B. Li, Y. Guo, L. Ye and Z. Lu, *RSC Advances*, 2017, **7**, 25469–25474.

[2] G. P. M. Poppe and C. M. J. Wijers, *ACM Trans. Math. Softw.*, 1990, **16**, 38–46.

[3] V. N. Faddeeva, N. M. Terent'ev, V. Fok, D. G. Fry and B. A. Hons, *Gosud. Izdat. Teh.-Teor. Lit. Moscow.*, 1954.

[4] S. G. Johnson, *Faddeeva Package*, 2023, `http://ab-initio.mit.edu/wiki/index.php/Faddeeva_Package`.

[5] A. Pattammattel, R. Tappero, M. Ge, Y. S. Chu, X. Huang, Y. Gao and H. Yan, *Science Advances*, 2020, **6**, 7.

[6] A. Pattammattel, R. Tappero, D. Gavrilov, H. Zhang, P. Aronstein, H. J. Forman, P. A. O'Day, H. Yan and Y. S. Chu, *Metallomics*, 2022, **14**, 11.